Radiation of acoustic and gravity waves and propagation of boundary waves in the stratified fluid from a time-varying bottom boundary

SHINGO WATADA[1]

[1]Earthquake Research Institute, University of Tokyo, Bunkyo-ku Yayoi 1-1-1, Tokyo 113-0032, Japan

(Received 8 January 2009)

Energy flow and radiation of linearized acoustic-gravity waves and propagation of boundary waves in a gravitationally stratified isothermal compressible inviscid semi-infinite fluid from a time-varying bottom boundary are investigated in the frequency-wavenumber domain. Impedance Z, the ratio of the bottom vertical displacement to the fluid pressure above it, is a function of the frequency and horizontal wavenumber (ω, k) of the bottom boundary undulation. The amplitude and phase of Z at the bottom boundary divide the (ω, k) coordinates into wavetype regimes. In contrast to the pure acoustic or gravity wave case, the phase of Z is continuous, but changes quickly across the regime boundaries between the propagating waves and trapped waves at the bottom, except for the Lamb wave branch along which the amplitude is infinite and across which the phase jumps by π. The phase of Z determines the efficiency of the work against the fluid by the deforming bottom boundary, showing reduced upward wave energy flow from the bottom near the regime boundaries where the phase of Z approaches $\pm\pi/2$. For precise modeling of pressure waves and the energy flow of acoustic and gravity waves in the fluid originat-

ing from a time-dependent bottom surface deformation with an apparent phase velocity comparable to the speed of sound in the fluid, it is necessary to include the dependency on (ω, k) of impedance Z.

---

1. Introduction

Low-frequency acoustic-gravity waves are generated from a bottom deformation of the atmosphere by events such as crustal deformation, seismic waves at the surface, and tsunamis associated with large earthquakes. Watada *et al.* (2006) observed atmospheric-scale air-ground coupling phenomena with collocated seismometers and microbarometers, confirming that simple acoustic phase and amplitude relationships between the pressure fluctuation and the seismic ground motion exists for a period up to 50 sec. At the same time, they also found theoretically that the air-ground coupling relation would deviate significantly from the simple acoustic one at around the acoustic cutoff frequency in a gravitationally stratified atmosphere.

In that study, the time-dependent topographic variation accompanying seismic waves was modeled as traveling waves whose constant horizontal phase speed is faster than the sound waves in air. For a purely acoustic case impedance Z, the spectral ratio of the bottom vertical velocity to the atmospheric pressure above it, is a function of the horizontal phase velocity of the deforming bottom boundary. In contrast to a pure acoustic case, impedance Z under gravity changes its amplitude and phase as functions of the horizontal wavenumber and the frequency of the time-varying bottom boundary undulation.

Radiating and trapped waves are generated from the motion of the bottom boundary in a gravitationally stratified compressible fluid. Golitsyn & Klyatskin (1967) studied the problem for radiating acoustic and gravity waves. Gravity waves in a stratified fluid, such as Lee waves or mountain waves, are generated from a moving bottom boundary with a topography, and are a special case of more general time-dependent bottom boundaries. Detailed histories of the study of Lee wave can be found in, for example, Gossard-Hooke (1975); Yih (1980); Baines (1995). On the other hand, we have rich examples of laboratory-scale application of radiating and evanescent acoustic waves at the boundary (Williams 1999) without taking into account the effect of gravity. Few studies have focused on the acoustic-gravity wave excitation problem by the more general time-varying atmospheric bottom boundary for a gravitationally stratified atmosphere. Golitsyn & Klyatskin (1967) studied the radiating acoustic-gravity waves from the time-varying atmospheric bottom boundary, but little discussed evanescent waves including Lamb waves.

The present report shows that the amplitude and phase of Z characterize both trapped and radiating waves, including acoustic, gravity, and Lamb waves, in a stratified isothermal fluid generated by the time-dependent bottom topography. Emphasis is placed to show the continuous transition of Z in the frequency-wavenumber domain from radiating waves to trapped waves including Lamb waves. A radiating wave is sometimes called an internal wave or free wave. A trapped wave is an external wave, evanescent wave, or boundary wave. The wave energy is concentrated near the "boundary" and decays exponentially in one direction. We also show that the vertical energy flow of acoustic-gravity waves is closely connected with the phase of Z.

In this study, the horizontal phase velocity of the time-dependent bottom boundary can be faster or slower than the sound waves and/or gravity waves in the fluid. Note that in this study neither fluid nor boundary elements move as fast as the the speed of sound in the fluid. Only the wave phase speed exceeds the speed of sound.

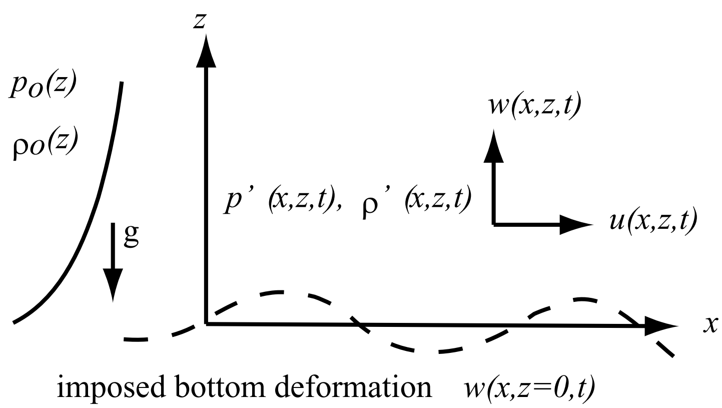

FIGURE 1. Problem geometry

2. Formulation

We investigate the mechanical coupling between the linear waves in a semi-infinite compressible stratified fluid and the bottom boundary in motion. Fluid particle velocity is assumed to be much smaller than the phase velocity of waves. We assume an isothermal inviscid fluid underlain by a flat horizontal bottom boundary where a time-dependent displacement field is imposed. The background fluid body is assumed to be at rest and not under rotation. Fluid viscosity is neglected. Energy transport by the heat conduction and radiation processes is not taken into account. Gill (1982) is followed in the first few sections to clarify the derivation including the scaling convention of variables. For example, Houghton (1986) adopts a different scaling convention. The new developments in this paper start at § 2.4.

We take positive x and z axes along the horizontal and vertical upward directions. t denotes the time, (u, w) are the horizontal and vertical components of fluid velocity, $\rho = \rho_o(z) + \rho'(x, z, t)$ and $p = p_o(z) + p'(x, z, t)$ are the density and pressure fields each of which is expressed as the sum of the background vertical profile and a small Eulerian perturbation (figure 1). We start with the linear momentum and mass conservation laws and the expression of adiabatic compression of the fluid. Neglecting the products of small quantities, including horizontal and vertical fluid velocities and the perturbations of density and pressure, we obtain

$$\rho_o \frac{\partial u}{\partial t} = -\frac{\partial p'}{\partial x} \tag{2.1a}$$

$$\rho_o \frac{\partial w}{\partial t} = -\frac{\partial p'}{\partial z} - \rho' \mathrm{g} \tag{2.1b}$$

$$\frac{\partial \rho'}{\partial t} + \frac{\partial(\rho_o u)}{\partial x} + \frac{\partial(\rho_o w)}{\partial z} = 0 \tag{2.2}$$

$${c_s}^2 = \left(\frac{\partial p}{\partial \rho}\right)_s , \tag{2.3}$$

equation 2.3 can be rewritten in terms of Lagrangian perturbations as

$${c_s}^2 \frac{\partial \delta\rho}{\partial t} = \frac{\partial \delta p}{\partial t}, \tag{2.4}$$

where g is the constant gravity and $c_s(z)$ is the speed of sound. In terms of Eulerian perturbations, the above equation is

$${c_s}^2 \left(\frac{\partial \rho'}{\partial t} + w\frac{d\rho_o}{dz}\right) = \frac{\partial p}{\partial t} + w\frac{dp_o}{dz} = \frac{\partial p'}{\partial t} - w\rho_o\, \mathrm{g}. \tag{2.5}$$

$\rho_o(z)$ and $p_o(z)$ satisfy the background state

$$\frac{dp_o}{dz} = -\rho_o\, \mathrm{g}. \tag{2.6}$$

Eliminating ρ' from equation 2.1, 2.2, and 2.5, we obtain the relationship between the Eulerian pressure perturbation p' and vertical upward velocity w as

$$\rho_o \frac{\partial}{\partial t}\left(\frac{\partial}{\partial z} - \frac{\mathrm{g}}{{c_s}^2}\right) w = \left(\frac{\partial^2}{\partial x^2} - \frac{1}{{c_s}^2}\frac{\partial^2}{\partial t^2}\right) p', \tag{2.7a}$$

$$\left(\frac{\partial^2}{\partial t^2} + N^2\right) w = -\frac{1}{\rho_o}\frac{\partial}{\partial t}\left(\frac{\partial}{\partial z} + \frac{\mathrm{g}}{{c_s}^2}\right) p', \tag{2.7b}$$

where buoyancy frequency N for a compressible fluid is defined by

$$[N(z)]^2 = -\mathrm{g}\left(\frac{1}{\rho_o}\frac{d\rho_o}{dz} + \frac{\mathrm{g}}{{c_s}^2}\right). \tag{2.8}$$

By scaling the horizontal and vertical ground velocities and pressure perturbation as

$$U = {\rho_o}^{1/2} u, W = {\rho_o}^{1/2} w, P = {\rho_o}^{-1/2} p', \tag{2.9}$$

we obtain a set of equations

$$\frac{\partial U}{\partial t} = -\frac{\partial P}{\partial x}, \tag{2.10a}$$

$$\frac{\partial}{\partial t}\left(\frac{\partial}{\partial z} W - \Gamma W\right) = \left(\frac{\partial^2}{\partial x^2} - \frac{1}{{c_s}^2}\frac{\partial^2}{\partial t^2}\right) P, \tag{2.10b}$$

$$\frac{\partial^2}{\partial t^2} W + N^2 W = -\frac{\partial}{\partial t}\left(\frac{\partial P}{\partial z} + \Gamma P\right), \tag{2.10c}$$

where Γ is defined by

$$\Gamma(z) = \frac{1}{2\rho_o}\frac{d\rho_o}{dz} + \frac{g}{{c_s}^2}. \tag{2.11}$$

These equations are often found in textbooks (e.g. Gossard-Hooke 1975). Note that Γ should not be confused with the adiabatic lapse rate. Both Γ and N^2 can be positive, negative, or zero, depending on the stratification of the compressible fluid (Beer 1974). The wave energy equation is derived from linearized equations 2.1, 2.2, and 2.5 (Gill 1982, p.170)

$$\frac{\partial}{\partial t}\left[\frac{1}{2}\rho_o(u^2 + w^2) + \frac{1}{2}\frac{p'^2}{\rho_o {c_s}^2} + \frac{1}{2}\rho_o N^2 h^2\right] + \frac{\partial}{\partial x}(p'u) + \frac{\partial}{\partial z}(p'w) = 0, \tag{2.12}$$

where h is vertical displacement defined by $h = \int w\, dt$. We denote the inside of [] in equation 2.12 as E, the wave energy density per unit volume including the kinetic and acoustic energy and energy associated with buoyancy. Equation 2.12 is rewritten as an energy conservation law (Lighthill 1978, p.294)

$$\partial E/\partial t + \boldsymbol{\nabla} \cdot \boldsymbol{I} = 0 \tag{2.13}$$

where the wave energy flow vector $\boldsymbol{I}$ is defined by

$$\boldsymbol{I} = (p'u, p'w). \tag{2.14}$$

The wave energy flow and density have a general relationship with each other through group velocity vector $\boldsymbol{v_g}$ of dispersive waves (Whitham 1974, p.386) that

$$\boldsymbol{I} = E\boldsymbol{v_g}. \tag{2.15}$$

Equation 2.15 is a convenient expression with which to evaluate the energy flow transported by the waves. In the following sections this equation is confirmed to hold for acoustic-gravity waves in a gravitationally stratified isothermal atmosphere.

2.1. *Isothermal atmosphere*

Hereafter we consider an artificial isothermal atmosphere as an example of stratified compressible fluid. Sound velocity c_s becomes constant for an isothermal atmosphere. Let $\gamma = c_p/c_v$ be the ratio of specific heat of the dry atmosphere, where c_p and c_v are the specific heat at constant pressure and constant volume, respectively. For an isothermal gravitationally stratified atmosphere with a constant scale height $\mathrm{H} = \mathrm{c_s}^2/\gamma\mathrm{g}$, buoyancy frequency N is a constant number expressed from equation 2.8 as

$$\mathrm{N}^2 = \mathrm{g}\left(\frac{1}{\mathrm{H}} - \frac{\mathrm{g}}{\mathrm{c_s}^2}\right), \tag{2.16}$$

and Γ in equation 2.11 is also a constant written as

$$\Gamma = \frac{1}{2\mathrm{H}} - \frac{\mathrm{N}^2}{\mathrm{g}} = \frac{1}{2}\left(\frac{\mathrm{g}}{\mathrm{c_s}^2} - \frac{\mathrm{N}^2}{\mathrm{g}}\right). \tag{2.17}$$

The last identity is obtained by eliminating H using in equation 2.16. Other miscellaneous expressions are found in appendix A.

2.2. *Dispersion relation*

Scaled pressure P and scaled horizontal and vertical velocities (U, W) have a plane-wave solution with a common angular frequency and wavenumber in the form $\exp\left(\mathrm{i}(kx + mz - \omega t)\right)$. Substituting these in equation 2.10 leads to equations

$$\omega U = kP, \tag{2.18a}$$

$$\omega(m + \mathrm{i}\Gamma)W = \left(\frac{\omega^2}{\mathrm{c_s}^2} - k^2\right) P, \tag{2.18b}$$

$$(\omega^2 - \mathrm{N}^2)W = \omega(m - \mathrm{i}\Gamma)P, \tag{2.18c}$$

from which we obtain the dispersion relation of waves in the atmosphere in the form

$$\mathrm{c_s}^{-2}\omega^4 - \omega^2(k^2 + m^2 + \mathrm{N}^2/\mathrm{c_s}^2 + \Gamma^2) + k^2\mathrm{N}^2 = 0, \tag{2.19}$$

or equivalently,

$$m^2 = \left(k^2 - \frac{\omega^2}{\mathrm{c_s}^2}\right)\left(\frac{\mathrm{N}^2}{\omega^2} - 1\right) - \Gamma^2. \tag{2.20}$$

This is also written as (Houghton 1986, p.108)

$$m^2 = k^2\left(\frac{\mathrm{N}^2}{\omega^2} - 1\right) + \frac{\omega^2 - \omega_\mathrm{a}{}^2}{\mathrm{c_s}^2}, \tag{2.21}$$

where the acoustic cutoff frequency ω_a is defined by

$$\omega_\mathrm{a}{}^2 = \mathrm{N}^2 + \mathrm{c_s}^2\Gamma^2. \tag{2.22}$$

Using equations 2.16 and 2.17, ω_a turns out to be

$$\omega_\mathrm{a} = \frac{\mathrm{c_s}}{2\mathrm{H}}. \tag{2.23}$$

2.3. *Group velocity*

We evaluate vertical wavenumber m by equation 2.20 or 2.21 for a given (ω, k) pair. (ω, k) as well as m^2 are assumed to be real. Negative and positive m^2 correspond to propagating waves and evanescent waves in the vertical direction, respectively. The sign of m is chosen from a physical consideration of the direction of the group velocity of the waves.

For evanescent waves in regimes E+ and E- of figure 2, group velocity is not defined from the dispersion relation in equation 2.20. In these regimes, since the vertical wavenumber is imaginary, all fluid elements in a vertical column move with the same

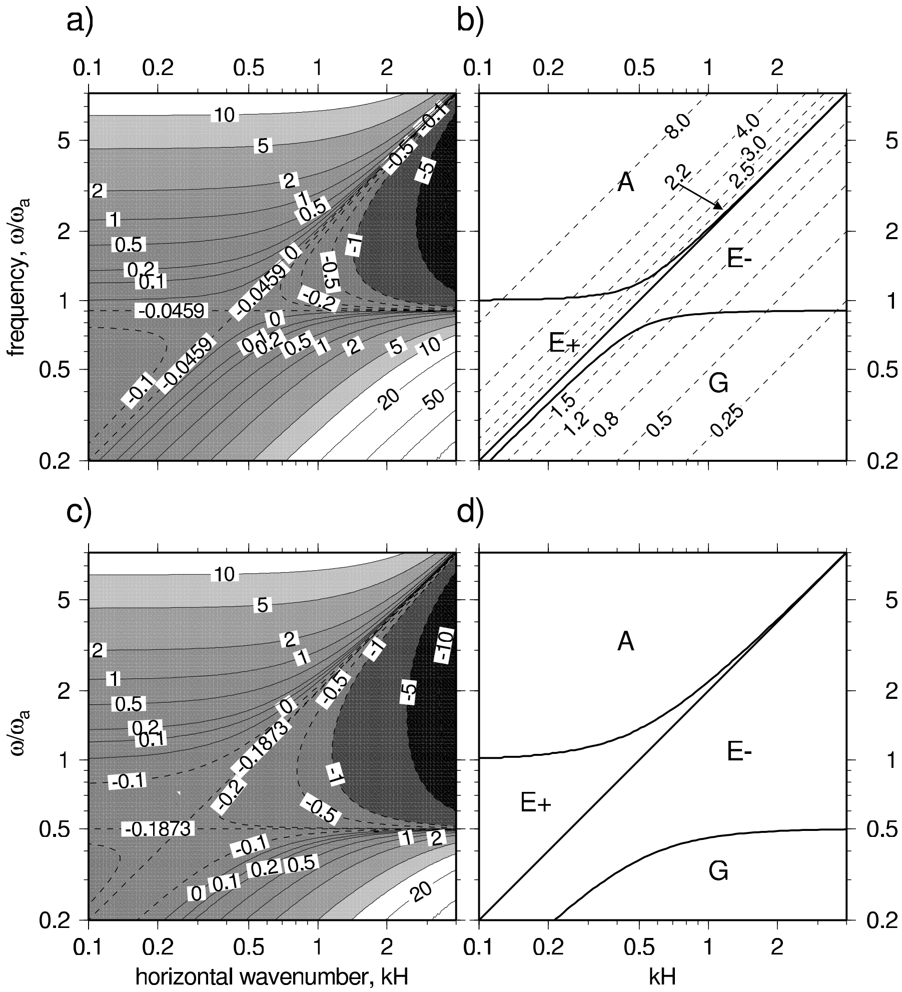

FIGURE 2. Wavenumber-frequency regimes characterised by $(m\mathrm{H})^2$. Abscissas are horizontal wavenumber k normalized by scale height H, ordinates are angular frequency ω normalized by the acoustic cutoff frequency ω_a. a) Contour map of the square of the normalized vertical wavenumber, $(m\mathrm{H})^2$, as a function of the normalized horizontal wavenumber and normalized frequency expressed by equations 2.20 and 2.21 with constants in appendix A. b) Regimes A, G, E+, and E- are separated along $m^2 = 0$ and $m^2 = -\Gamma^2$ lines. Dashed lines are along constant horizontal phase speeds, normalized by $\omega_\mathrm{a}\mathrm{H} = \mathrm{c_s}/2$. Thus normalized phase speed 2 corresponds to $\mathrm{c_s}$, the speed of sound. m^2 are positive in regimes A and E and negative in regimes E+ and E-. Regimes E+ and E- are separated along a constant phase line $(\omega/\omega_\mathrm{a})/(k\mathrm{H}) = 2$ along which $m^2 = -\Gamma^2$. c), d) same to figure a) and b) for a non-isothermal case in which $\omega_\mathrm{a} = 0.5N$. c) and d) are only for illustration purpose and are not discussed further.

phase and no waves propagate vertically. In the horizontal direction, the wave phase is $(kx-\omega t)$, the same as the bottom imposed deformation. The phase speed ω/k and group speed $\partial\omega/\partial k$ are also the same as those of the bottom-imposed deformation, and are not calculated from the wave dispersion relations in equation 2.20.

The group velocity of propagating waves in the gravitationally stratified isothermal atmosphere is formally expressed from equations 2.19 and 2.21

$$\mathbf{v_g} = ({v_g}_x, {v_g}_z) = \left(\frac{\partial\omega}{\partial k}, \frac{\partial\omega}{\partial m}\right) = \frac{{\mathrm{c_s}}^2\omega}{\omega^4 - k^2\mathrm{N}^2{\mathrm{c_s}}^2}\left(k(\omega^2-\mathrm{N}^2), m\,\omega^2\right). \qquad (2.24)$$

The sign of v_{gz}, the vertical component of group velocity, is determined by the denominator in equation 2.24 and m. When the denominator $\omega^2 - k\mathrm{Nc_s} = 0$, the sign of m^2 is always negative, since from equation 2.20 and $\omega^2 = k\mathrm{Nc_s}$, the following inequation holds

$$m^2(\omega,k) = \left(k^2 - \frac{k\mathrm{Nc_s}}{{\mathrm{c_s}}^2}\right)\left(\frac{\mathrm{N}^2}{k\mathrm{Nc_s}} - 1\right) - \Gamma^2 = -\left(k - \frac{\mathrm{N}}{\mathrm{c_s}}\right)^2 - \Gamma^2 < 0. \qquad (2.25)$$

This inequation proves that in the (ω, k) coordinates, the entire $\omega^2 - k\mathrm{Nc_s} = 0$ line lies in the region of evanescent waves in the vertical direction, i.e., in regimes E+ and E-. Thus in regimes A and G, the group velocity defined by equation 2.24 takes non-zero finite values.

The wave energy propagates along the direction of the group velocity vector at the speed of the group velocity. In this study, we assume that wave energy is provided by the motion of the bottom boundary. If m is real the sign of v_{gz} must be always positive. In propagating acoustic wave regime A, the denominator of v_{gz} in equation 2.24 is positive and m in the numerator must also be positive. In propagating gravity wave regime G, the denominator of v_{gz} is negative and hence m in the numerator must also be negative.

In evanescent regimes E+ and E-, the energy is bounded toward the bottom boundary, and $\mathrm{i}\sqrt{-m^2}$ is the right choice between $\pm\mathrm{i}\sqrt{-m^2}$ for $m^2 < 0$ because we assume spatial dependency in the form of $\exp(\mathrm{i}mz)$.

2.4. *Wave energy*

Wave energy density E in 2.12 in both propagating acoustic regime A and gravity regime G is expressed with the scaled variables in equation 2.9 as

$$E(\omega, k) = \frac{1}{2}\left[UU^* + WW^* + \frac{PP^*}{\mathrm{c_s}^2} + \frac{\mathrm{N}^2}{\omega^2}WW^*\right] \tag{2.26a}$$

$$= PP^*\left(\frac{\mathrm{N}^2 k^2}{\omega^2} - \frac{\omega^2}{\mathrm{c_s}^2}\right)/(\mathrm{N}^2 - \omega^2) \tag{2.26b}$$

$$= WW^*\left(\frac{\mathrm{N}^2 k^2}{\omega^2} - \frac{\omega^2}{\mathrm{c_s}^2}\right)/\left(k^2 - \frac{\omega^2}{\mathrm{c_s}^2}\right). \tag{2.26c}$$

We have used equation 2.18 to eliminate U, P, and W. Each asterisk denotes the complex conjugate of the variable. Because horizontal wavenumber k and frequency ω are both real, energy density E is always real and no imaginary part exists for all (ω, k). See appendix B for details. The components of the wave energy flow in regimes A and G are computed from equations 2.24 and 2.26

$$E\, v_{gx} = \frac{k}{\omega}PP^* = PU^*, \tag{2.27a}$$

$$E\, v_{gz} = -\frac{m\omega}{\mathrm{N}^2 - \omega^2}PP^* = \frac{m}{m + i\Gamma}PW^* = \frac{m}{m - i\Gamma}P^*W$$

$$= Re(PW^*) = \frac{1}{2}(PW^* + P^*W). \tag{2.27b}$$

The wave energy flow, as we expected in equation 2.15, is the product of pressure and fluid velocity. Note that, if energy flow has a complex part, the observable quantity should be the real part of the complex variables (Blackstock 2000, p.49). Wave energy defined by equation 2.26 and wave energy flow defined by equation 2.27 have a $\cos^2(\omega t)$ dependence in time. After taking the average over a time period much longer than the wave period, the time dependence $\cos^2(\omega t)$ is replaced by $1/2$. P and U are always in phase, as seen from equation 2.18, and the horizontal energy flow PU^* is real. PW^* has an imaginary component expressing a phase shift between W and P for real $m(\omega, k)$ in regimes A and G. When $m(\omega, k)$ becomes imaginary in regimes E+ and E-, then P and W are in phase quadrature, i.e., the phases of two variables are shifted by $\pm\pi/2$, as seen in equation 2.18, implying that the pressure change is positively or negatively proportional to the vertical displacement, and that no energy flow exists in the vertical direction.

2.5. *Impedance*

Impedance Z, the ratio between the vertical velocity and pressure at the boundary, (also called transfer function in (Watada *et al.* 2006)), normalized by air density and the speed of sound, is derived from using equations 2.18 as

$$Z(\omega,k) \equiv \frac{p'}{\rho_o \mathrm{c_s} w} = \frac{P}{\mathrm{c_s} W} = \frac{2\omega/\omega_\mathrm{a}}{\frac{\omega^2}{{\omega_\mathrm{a}}^2} - 4k^2\mathrm{H}^2}\mathrm{H}\left(D(m) + \mathrm{i}\Gamma\right) \tag{2.28a}$$

$$= \frac{(\omega^2 - N^2)/{\omega_\mathrm{a}}^2}{2\frac{\omega}{\omega_\mathrm{a}}\mathrm{H}(D(m) - \mathrm{i}\Gamma)}. \tag{2.28b}$$

The last identity is verified from the dispersion relation in equation 2.20. $D(m)$ is defined by

$$D(m) = \begin{cases} \sqrt{m^2} & \text{for regime A} \\ -\sqrt{m^2} & \text{for regime G} \\ \mathrm{i}\sqrt{-m^2} & \text{for regimes E+, E-} \end{cases} \tag{2.29}$$

corresponding to propagating acoustic waves, propagating gravity waves, and trapped waves along the bottom boundary in descending order in equation 2.29, respectively. The sign of $D(m)$ is chosen as discussed in §2.3. Because propagating gravity waves with energy flow upward in an incompressible fluid have the relationship (see appendix C)

$$\frac{p'}{\rho_o w} = \frac{\mathrm{N}}{k}\sqrt{1 - \left(\frac{\omega}{\mathrm{N}}\right)^2}\ , \tag{2.30}$$

another nondimensional impedance is defined

$$Z'(\omega,k) \equiv \frac{kp'}{\rho_o \mathrm{N} w} = \frac{k}{\mathrm{N}}\frac{P}{W} = \frac{2\omega_\mathrm{a} k\mathrm{H}}{\mathrm{N}} Z(\omega,k). \tag{2.31}$$

This form of impedance in equation 2.31 would be suited for the study of propagating gravity wave in region G, where impedance expressed by Z' in equation 2.31 is flat compared with the one expressed by impedance Z in equation 2.28. The impedance normalization factors — $1/(\rho_o c_s)$ for propagating acoustic waves and $k/(\rho_o N)$ for propagating gravity waves — will also be justified by the study of asymptotic forms of impedance in § 3.1.2. Two impedance expressions are correct for all (ω, k) and the choice between equation 2.28 and 2.31 depends on the problem to study.

Watada *et al.* (2006) examined only seismic waves and obtained the transfer function of regimes A and E+, the horizontal phase velocity of the bottom boundary deformation is faster than the speed of sound in air. The result of Watada *et al.* (2006) cannot be applied to the radiation of gravity waves from the bottom boundary (equation 2.29). Equation 2.28, or 2.31, is the basic equation of this paper and is used to compute the impedance for all (ω, k). The positive and negative signs in equation 2.29 for acoustic and gravity waves should be taken into account in modeling the pressure waves in the atmosphere induced by the time-varying bottom boundary. The phase and amplitude of impedance in equation 2.28, together with the wave types, are discussed in detail in the next section.

3. Results

3.1. *Impedance*

The functional form of equations 2.28 and 2.29 exhibits a few features of impedance $Z(\omega, k)$. First, the amplitude of the impedance becomes infinite when the horizontal phase velocity ω/k is equal to the speed of sound $c_s = 2H\omega_a$ in a fluid, i.e., Lamb waves, for all wavelengths. No vertical motion exists and the phase of Z is indefinite in Lamb waves. Across the Lamb wave branch, the phase of Z jumps by π. Second, the amplitude of impedance is reduced, but not zero along the $m = 0$ lines, which are the regime boundaries between propagating waves and trapped waves. Third, the phase of Z

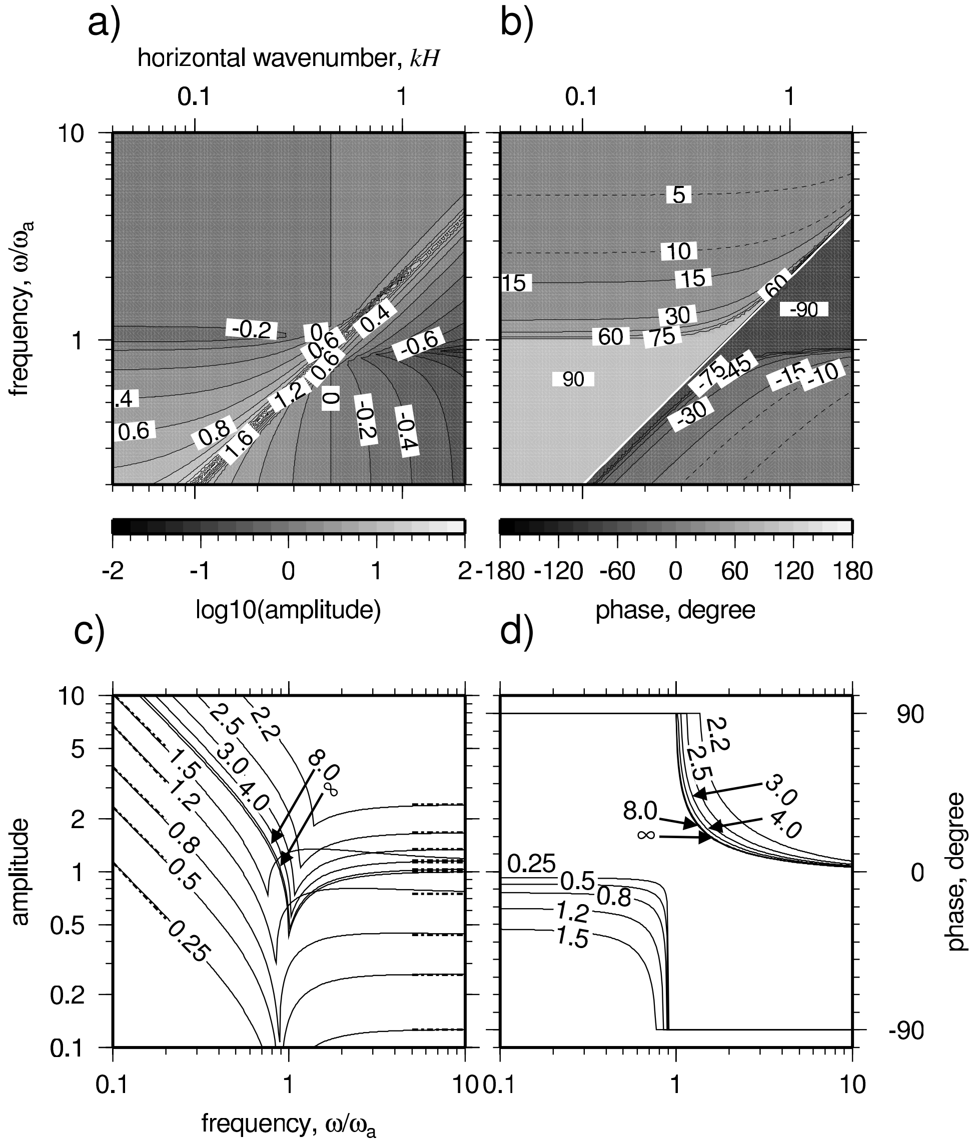

FIGURE 3. Theoretical impedance for an isothermal atmosphere, as expressed in equation 2.28. a) and b) are contour maps of the amplitude and phase of the impedance, respectively. In c) and d), amplitude and phase are evaluated along the constant horizontal phase speed lines in figure 2, respectively. The dashed short lines near frequencies 0.1 and 10.0 in figure c indicate the asymptotic value of each constant phase speed in table 2.

is determined by $D(m)$ because Γ is a constant value for an isothermal atmosphere. The vertical wavenumber m is constant along the constant phase line of Z. For all $m^2 \leqslant 0$

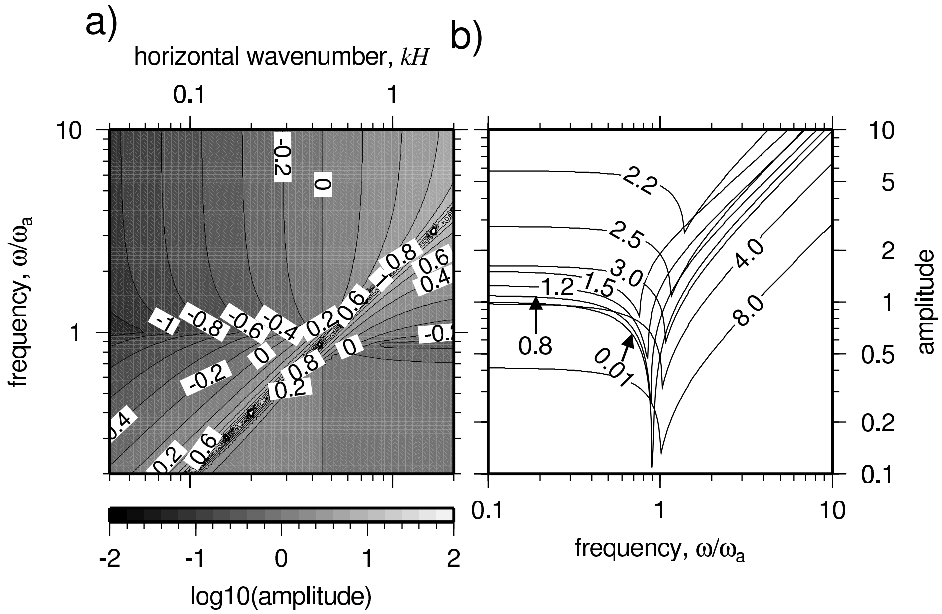

FIGURE 4. Theoretical impedance expressed in equation 2.31. a) Contour map of amplitude, b) amplitude along constant horizontal phase speeds. The phase plot is the same as in figure 3b).

the phase of Z becomes a constant value — $\pi/2$ or $-\pi/2$ — depending upon regime E+ or E-, respectively. Pressure change and vertical displacement are in phase and out of phase, in regime E+ and in regime E-, respectively.

In figures 3 and 4 impedance Z as a function of the horizontal wavenumber and frequency of a time-dependent bottom boundary is plotted for an isothermal atmosphere, using the atmosphere-like parameters in appendix A. The plot confirms the features described above. The phase of impedance Z is continuous across the regime boundaries along $m = 0$ between the propagating wave and the trapped wave, i.e., across the boundary between A and E+ and that between G and E-.

3.1.1. *Comparison with a pure acoustic wave case and an incompressible gravity wave case*

For purely acoustic waves, $m = 0$ corresponds to the waves propagating in the direction parallel to the bottom boundary at the speed of sound. If the horizontal phase speed of the time-dependent boundary undulation changes slightly near the speed of sound, the phase of the induced pressure relative to the phase of the bottom boundary deformation jumps abruptly by $\pi/2$. For acoustic waves with a horizontal phase speed faster than the speed of sound, i.e., vertically and horizontally propagating waves, bottom pressure and vertical upward velocity are in phase. For vertically evanescent acoustic waves with a horizontal phase speed slower than the speed of sound, bottom pressure and vertical upward displacement are out of phase.

For incompressible waves under gravity, $m = 0$ corresponds to the purely vertical motion of an entire vertical column at buoyancy frequency N. The bottom pressure and vertical upward velocity of the bottom boundary are in phase below the buoyancy frequency, and bottom pressure and vertical displacement are out of phase above the buoyancy frequency. By crossing the buoyancy frequency, we encounter a bump by $\pi/2$ in the phase of Z.

The combined effects of compressibility and stratification cause the impedance phase steps to disappear in the (ω, k) coordinates, except for the Lamb wave branch. Figure 3-d shows the continuous transition of the phase of Z across the regime boundaries along various constant horizontal phase speed lines.

3.1.2. *Asymptotic forms of impedance*

Impedance in equation 2.28 should have simple asymptotic forms by taking the limits of the variables (ω, k). By assuming $|m^2| \gg \Gamma$, we approximate equations 2.20 and 2.18 to obtain

$$\omega m W = \left(\frac{\omega^2}{\mathrm{c_s}^2} - k^2\right) P \tag{3.1a}$$

$$(\omega^2 - \mathrm{N}^2) W = \omega m P \tag{3.1b}$$

	Regime A	Regime G	Regime E+	Regime E-
$\frac{P}{c_s W} = \frac{p'}{c_s \rho_o w} =$	$\sqrt{\frac{1-\left(\frac{N}{\omega}\right)^2}{1-\left(\frac{c_s}{\omega/k}\right)^2}}$	$\sqrt{\frac{\left(\frac{N}{\omega}\right)^2-1}{\left(\frac{c_s}{\omega/k}\right)^2-1}}$	$i\sqrt{\frac{\left(\frac{N}{\omega}\right)^2-1}{1-\left(\frac{c_s}{\omega/k}\right)^2}}$	$-i\sqrt{\frac{1-\left(\frac{N}{\omega}\right)^2}{\left(\frac{c_s}{\omega/k}\right)^2-1}}$
$=$	$\frac{N}{kc_s}\sqrt{\frac{\left(\frac{\omega}{N}\right)^2-1}{\left(\frac{\omega/k}{c_s}\right)^2-1}}$	$\frac{N}{kc_s}\sqrt{\frac{1-\left(\frac{\omega}{N}\right)^2}{1-\left(\frac{\omega/k}{c_s}\right)^2}}$	$i\frac{N}{kc_s}\sqrt{\frac{1-\left(\frac{\omega}{N}\right)^2}{\left(\frac{\omega/k}{c_s}\right)^2-1}}$	$-i\frac{N}{kc_s}\sqrt{\frac{\left(\frac{\omega}{N}\right)^2-1}{1-\left(\frac{\omega/k}{c_s}\right)^2}}$

TABLE 1. Approximated impedance for $|m^2| \gg \Gamma$

Limiting case	A	G	E+	E-
$\frac{N}{\omega}\to 0,\ \frac{c_s}{\omega/k} =$ finite	$\frac{1}{\sqrt{1-\left(\frac{c_s}{\omega/k}\right)^2}}$			$-i\frac{1}{\sqrt{\left(\frac{c_s}{\omega/k}\right)^2-1}}$
$\frac{c_s}{\omega/k}\to 0,\ \frac{N}{\omega} =$ finite	$\sqrt{1-\left(\frac{N}{\omega}\right)^2}$		$i\sqrt{\left(\frac{N}{\omega}\right)^2-1}$	
$\frac{N}{\omega}\to \infty,\ \frac{c_s}{\omega/k} =$ finite		$\frac{N}{kc_s}\frac{1}{\sqrt{1-\left(\frac{\omega/k}{c_s}\right)^2}}$	$i\frac{N}{kc_s}\frac{1}{\sqrt{\left(\frac{\omega/k}{c_s}\right)^2-1}}$	
$\frac{c_s}{\omega/k}\to \infty,\ \frac{N}{\omega} =$ finite		$\frac{N}{kc_s}\sqrt{1-\left(\frac{\omega}{N}\right)^2}$		$-i\frac{N}{kc_s}\sqrt{\left(\frac{\omega}{N}\right)^2-1}$

TABLE 2. Asymptotic forms of impedance

and a dispersion relation

$$m^2 = \left(\frac{\omega^2}{{c_s}^2} - k^2\right)\left(1 - \frac{N^2}{\omega^2}\right). \tag{3.2}$$

Using approximated equations 3.1 and 3.2, and the same discussion of the sign of m in § 2.3, we rewrite the impedance in equation 2.28 to obtain table 1. Further, we obtain asymptotic forms of impedance for the limiting cases of variables N/ω and $c_s k/\omega$ (table 2).

Figure 3-c shows that the impedance amplitude approaches the values calculated from the asymptotic forms in table 2 as the frequency increases and decreases along constant horizontal phase speed lines. The phase approaches 0 or $\pm\pi/2$, depending upon the regimes in figure 2-b.

Note that the impedance normalization factors used in equations 2.28 and 2.30 correspond to the limiting cases of regime A with $\mathrm{N}/\omega \to 0, \mathrm{c_s}/(\omega/k) \to 0$, and regime G with $\mathrm{N}/\omega \to \infty, \mathrm{c_s}/(\omega/k) \to \infty$, respectively.

3.2. *Scale height*

Eulerian pressure perturbation p' and velocity (u, w) are expressed using $D(m)$ in equation 2.29

$$p' = \rho_o^{1/2} P = P_o \rho_{oo}^{1/2} \exp(-z/2\mathrm{H}) \exp(\mathrm{i}(kx + D(m)z - \omega t)) \tag{3.3}$$

$$(u, w) = \rho_o^{-1/2}(U, W) = (U_o, W_o)\rho_{oo}^{-1/2} \exp(+z/2\mathrm{H}) \exp(\mathrm{i}(kx + D(m)z - \omega t)) \tag{3.4}$$

where P_o and (U_o, W_o) are constant scaled pressure and velocity at the boundary, respectively. $\rho_o(z) = \rho_{oo} \exp(-z/\mathrm{H})$, ρ_{oo} is the density of the atmosphere at the bottom surface.

In propagating wave regimes, scale height is constant. In evanescent regimes, scale height changes depending on the m^2 value in figure 2-a. If $(mH)^2 > -1/4$ is satisfied for an evanescent wave, as altitude increases the wave energy density decreases but the wave velocity increases exponentially. Thus, evanescent waves can be observed at high altitude as a large fluid velocity perturbation. Along Lamb waves, m^2 is constant $-\Gamma^2$. The Lamb waves can be considered as a special case of boundary waves without boundary deformation.

3.3. *Work and energy flow by bottom stress*

In propagating regimes A and G, the pressure p' and horizontal fluid velocity u are in phase and there is always a wave energy flow along the boundary expressed by $\overline{p'u}/2$, where the overscore is the time average of the variable. Since

$$\frac{P}{W} = \frac{PW^*}{WW^*} \tag{3.5}$$

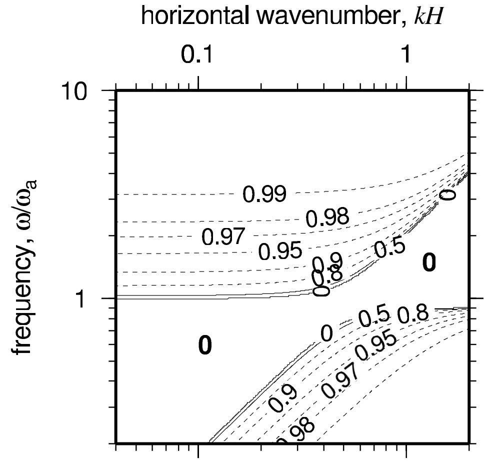

FIGURE 5. Vertical energy flow efficiency defined by $\overline{p'w}/\sqrt{\overline{p'^2}\ \overline{w^2}}$.

holds, the phase of $p'w$ is the same as that of impedance Z in equation 2.28 and will be evaluated for all (ω, k). Compared with a pure acoustic or gravity wave case, the vertical energy flow expressed by $\overline{p'w}$ has reduced efficiency near the regime boundaries because the phase difference between p' and w comes close to being shifted by $\pm\pi/2$ (figures 3-b, 5).

In evanescent regimes E+ and E-, horizontal energy flow $\overline{p'u}$ exists but vertical energy flow completely vanishes because p' and w are in quadrature and bottom deformation does not work against the atmosphere above it. Physically, the undulating bottom boundary horizontally stretches and shortens the atmospheric bottom layer locally within the depth of the scale height and temporally within the timescale of the wave period. The horizontal wavenumber and the frequency of the undulating boundary do not satisfy the conditions for the propagating waves $m^2 \geqslant 0$, thus only boundary waves are generated.

4. Concluding remarks

A real gravitationally stratified fluid, such as atmosphere, is not isothermal. In such a fluid, temperature decreases or increases as altitude increases, and the dispersion relation of internal and external waves will be altered from that of an isothermal fluid (Beer 1974). A shear flow will also change the propagation of waves. Studies of internal gravity waves in a Boussinesq inviscid adiabatic fluid revealed that gravity waves are dissipated and reflected at a critical height with a shear flow (Booker & Bretherton 1967). The present study does not consider shear flow. The realistic stratification of the temperature (or buoyancy frequency $N(z)$) and wind speed in the atmosphere is known to significantly change the forms of the dispersion branches and the boundaries between different regimes in the (ω, k) plane (e.g. Gossard-Hooke 1975). Shear flow and temperature effects on the propagation of radiated or trapped acoustic-gravity waves from the bottom boundary are left for future studies. Realistic temperature and density models of the atmosphere are needed to correctly compute the propagation of pressure disturbances.

Mountain wave analysis of a stratified incompressible fluid predicts that the relative phase between pressure and displacement changes by $\pi/2$ when the frequency crosses the $\omega = \mathrm{N}$ line (e.g. Gill 1982; Cushman-Roisin 1994). This study extends the mountain wave analysis for the cases of a horizontal phase speed of deformation larger or smaller than the speed of sound. For cases where the horizontal phase speed is below the speed of sound and the wave frequency is larger than the buoyancy frequency, this study shows that an upward deformation of the boundary causes a negative pressure change, similar to the case of the mountain waves that have a frequency larger than the buoyancy frequency. When the horizontal phase speed exceeds the speed of sound but the wave frequency is lower than the acoustic cutoff frequency, the upward deformation of the boundary accompanies a pressure increase. It should be noted that regimes E+ and E- have an infinite horizontal wavenumber and frequency range, both extending along the $(\omega/\omega_\mathrm{a})/(k\mathrm{H}) = 2$ regime boundary in figure 3. In regimes E+ and E-, pressure increases as the bottom boundary deforms upward and downward, respectively.

This study is limited to the linear waves. Under linear wave approximation, deep water surface gravity waves of the ocean is in regime E- and no vertical acoustic wave propagation is expected. Guo (1987), Arendt & Fritts (2000), and Waxler & Gilbert (2006) demonstrated, however, that acoustic waves in air can be radiated from ocean surface gravity waves through the nonlinear effects of surface waves. Linear approximation used in this paper may become invalid near the regime boundaries, where the horizontal phase speed becomes close to zero, for instance when ω is close to N and, therefore, comparable in value to the fluid particle velocities. The nonlinear case requires a particular consideration and imposes certain restrictions on the applicability of the linear approximation assumed in this study.

When we model the atmospheric waves generated by a tsunami, defined as a long gravity wave in the ocean whose horizontal phase velocity is less than the atmospheric speed of sound, the boundary condition at the ocean surface depends on where the tsunami dispersion branch goes in regimes G and E-. Long-period tsunami in regime G generates gravity waves in the atmosphere (Golitsyn & Klyatskin 1967). The boundary condition of atmospheric waves excited by seismic waves, whose horizontal propagation speed are in general faster than the atmospheric speed of sound, depends on the wave period. Waves with a frequency larger or smaller than the acoustic cutoff frequency are in regime A or E+, respectively. If an ocean depth were greater than 11000 m, then the phase speed of a tsunami would exceed the speed of sound in the atmosphere. The dispersion branch of this supersonic tsunami crosses the Lamb wave branch and the boundary condition of the supersonic tsunami switches to the same one for seismic waves.

The source of atmospheric acoustic-gravity waves excited by the deformation of the bottom boundary is often modeled as a pressure source at the bottom related by $p' = \rho_o \mathrm{c_s} w$ (e.g. Mikumo *et al.* 2008). This study shows that, in an isothermal atmosphere, this approximation is good only for acoustic waves with horizontal phase speed much faster than acoustic waves. The amplitude and phase of the pressure field above the deforming bottom depends on whether the horizontal phase speed is faster or slower than the speed of sound, and on whether the oscillation period is longer or shorter than the buoyancy period of the atmosphere. For precise modeling of the amplitude and phase of an atmospheric disturbance originated by a time-dependent bottom surface deformation imposed by seismic waves and tsunamis with a horizontal phase velocity comparable to the speed of sound in air, dependence on (ω, k) of impedance Z should be taken into account.

I would like to acknowledge the useful comments of Drs. S. Takehiro, H. Shimizu, and K. Nakajima. I thank an anonymous referee for bringing Golitsyn & Klyatskin (1967) to my attention. This research is supported by a Grant in Aid for Science Research (C) 18540413 from the Ministry of Education, Culture, Sports, Science, and Technology of Japan.

Appendix A. Miscellaneous expressions

Equation of the state of an ideal gas and adiabatic atmospheric process results in a relationship between the specific heat ratio γ, pressure p, density ρ, and speed of sound $\mathrm{c_s}$,

$$\mathrm{c_s}^2 = \frac{\gamma p}{\rho}. \qquad \text{(A 1)}$$

Derivations is found in textbooks (e.g. Gill 1982). In an isothermal atmosphere, a constant scale height H is defined by

$$\frac{1}{\mathrm{H}} = -\frac{1}{p}\frac{dp}{dz}. \qquad \text{(A 2)}$$

From equations A 1, 2.6, A 2, and $p = \rho \mathrm{R}T$ where R is the gas constant, speed of sound is rewritten as

$$\mathrm{c_s}^2 = \gamma \mathrm{R}T = \gamma \mathrm{gH}. \tag{A 3}$$

Thus the acoustic cutoff frequency ω_a, Γ, and the buoyancy frequency N are expressed using γ, H and g

$$\omega_\mathrm{a} = \frac{\mathrm{c_s}}{2\mathrm{H}} = \frac{1}{2}\sqrt{\frac{\gamma g}{\mathrm{H}}}, \tag{A 4a}$$

$$\mathrm{N}^2 = \mathrm{g}\left(\frac{1}{\mathrm{H}} - \frac{\mathrm{g}}{\mathrm{c_s}^2}\right) = \frac{(\gamma-1)\mathrm{g}}{\gamma \mathrm{H}} = \frac{4(\gamma-1)}{\gamma^2}\omega_\mathrm{a}{}^2, \tag{A 4b}$$

$$\Gamma = \frac{1}{2\mathrm{H}} - \frac{\mathrm{N}^2}{\mathrm{g}} = \frac{2-\gamma}{2\gamma \mathrm{H}}. \tag{A 4c}$$

For a diatomic gas, γ=1.4. If we adopt atmosphere-like parameters, H=8.0 km, g=9.8 m/s^2, R=287.04J/kg K, then ω_a, N=0.9035ω_a, and Γ are derived using equations A 4 and can be used to plot figures 2-5.

Appendix B. Computation of acoustic-gravity wave energy and wave energy flow

A wave is an oscillatory phenomenon in space and time and is often modeled as complex variables having exponential dependence in the form $\exp(\mathrm{i}(kx + mz - \omega t))$. Wave energy and energy flow are defined by the products of two variables, as seen in equations 2.12 and 2.14. The acoustic-gravity wave energy density per unit volume in equation 2.12 is expressed as

$$E(\omega, k, z) = \frac{1}{2}\left[\rho_o(uu^* + ww^*) + \rho_o N^2 hh^* + \frac{p'p'^*}{\rho_o \mathrm{c_s}^2}\right]. \tag{B 1}$$

With the scaled variables in equation 2.9, the wave energy density per unit volume equation B 1 for propagating waves (regimes A and G) is also written as

$$E(\omega, k) = \frac{1}{2}\left[UU^* + WW^* + \frac{PP^*}{\mathrm{c_s}^2} + \frac{\mathrm{N}^2}{\omega^2}WW^*\right]. \tag{B 2}$$

The z dependence of $E(\omega,k)$ disappears because of the scaling in equation 2.9. For evanescent waves (regimes E+ and E-) we adopt a different scaling of variables so that each term in equation B 1 has a common dependence on z.

$$U=\rho_{oo}{}^{M\mathrm{H}}\rho_o{}^{1/2-M\mathrm{H}}u,\ W=\rho_{oo}{}^{M\mathrm{H}}\rho_o{}^{1/2-M\mathrm{H}}w,\ P=\rho_{oo}{}^{M\mathrm{H}}\rho_o{}^{-1/2-M\mathrm{H}}p', \tag{B 3}$$

where $M{=}\sqrt{-m^2}$ and $\rho_{oo}{=}\rho_o(0)$. The complex conjugate of equation 2.18b gives

$$\mathrm{i}\omega(\mathrm{i}m^*+\Gamma)W^*=\left(\frac{\omega^2}{\mathrm{c_s}^2}-k^2\right)P^*. \tag{B 4}$$

From equations 2.18c and B 4 we have the following relations

$$(\mathrm{N}^2-\omega^2)(\mathrm{i}m^*+\Gamma)WW^*=\left(k^2-\frac{\omega^2}{\mathrm{c_s}^2}\right)(\mathrm{i}m+\Gamma)PP^*, \tag{B 5}$$

$$(-\omega^2+N^2)\left(k^2-\frac{\omega^2}{\mathrm{c_s}^2}\right)WP^*=-\omega^2(\mathrm{i}m+\Gamma)(\mathrm{i}m^*+\Gamma)PW^*. \tag{B 6}$$

Applying equations 2.18a and B 5 to equation B 2, for propagating waves m is real, we reach equation 2.26. For evanescent waves $\mathrm{i}m=-M$ is real, we reach

$$E(\omega,k,z)=\frac{1}{2}e^{-2Mz}\left[\frac{k^2}{\omega^2}+\frac{1}{\mathrm{c_s}^2}+\left(1+\frac{\mathrm{N}^2}{\omega^2}\right)\left(\frac{k^2-\omega^2/\mathrm{c_s}^2}{\mathrm{N}^2-\omega^2}\right)\left(\frac{-M+\Gamma}{M+\Gamma}\right)\right]PP^*, \tag{B 7}$$

which is also real. Thus, energy density is real for all (ω,k), and we do not need to take the real part of energy density. Wave energy flow defined by equation 2.14 is formally expressed as

$$\boldsymbol{I}(\omega,k)=\mathrm{Re}(p'u^*,p'w^*)=(PU^*,\mathrm{Re}(PW^*)). \tag{B 8}$$

From equation 2.18a, U and P are in phase so that horizontal wave energy flow PU^* is real for all (ω,k) and we do not take the real part of PU^*. Strictly speaking, P and W are not in phase for all (ω,k) so we should take the real part of PW^*.

Appendix C. Impedance for gravitationally stratified incompressible fluid

In a vertically stratified incompressible fluid with a constant buoyancy frequency N, the linearized equation of motion in the horizontal component is

$$\rho_o \frac{\partial u}{\partial t} = -\frac{\partial p'}{\partial x}. \tag{C 1}$$

The incompressibility is expressed as

$$\frac{\partial u}{\partial x} + \frac{\partial w}{\partial z} = 0. \tag{C 2}$$

By assuming a plane wave solution $\exp(\mathrm{i}(kx + mz - \omega t))$, we have

$$\omega \rho_o u = kp', \tag{C 3}$$

$$ku + mw = 0. \tag{C 4}$$

The dispersion relation of the incompressible fluid has a dispersion relation (Gill 1982, p131)

$$\omega^2 = \mathrm{N}^2 \frac{k^2}{k^2 + m^2}. \tag{C 5}$$

After considering the sign of m as we discussed in §2.3, we have for gravity waves propagating upward

$$m = -k\sqrt{1 - \left(\frac{\omega}{\mathrm{N}}\right)^2}\,. \tag{C 6}$$

From equations C 3, C 4, and C 6, we have equation 2.30.

REFERENCES

ARENDT, S. & D. C. FRITTS 2000 Acoustic radiation by ocean surface waves. *J. Fluid Mech.* **415**, 1–21.

BAINES, P. G. 1995 *Topographic Effects in Stratified Flows.* Cambridge Univ. Press.

BEER, T. 1974 *Atmospheric Waves.* Adam Hilger, London.

BLACKSTOCK, D. T. 2000 *Fundamentals of Physical Acoustics.* John Wiley & Sons.

Booker, J. R. & Bretherton, F. P. 1967 The critical layer for internal gravity waves in a shear flow. *J. Fluid Mech.* **27**, 513–539.

Cushman-Roisin, B. 1994 *Introduction to Geophysical Fluid Dynamics.* Prentice-Hall.

Gill, A. E. 1982 *Atmosphere-Ocean Dynamics.* Elsevier.

Golitsyn, G. S., & Klyatskin, V. I 1967 Atmospheric oscillations caused by movements of Earth's surface. *Izv. Atmos. Ocean. Phys.* **3**, 613–617.

Gossard, E. E., & Hooke, W. H. 1975 *Waves in the Atmosphere.* Elsevier.

Guo, Y. P. 1987 Waves induced by source near the ocean surface. *J. Fluid Mech.* **181**, 293–310.

Houghton, J. T. 1986 *The Physics of Atmosphere.* 2nd ed., Cambridge Univ. Press.

Lighthill, J. 1978 *Waves in Fluids.* Cambridge Univ. Press.

Mikumo, T. & Shibutani, T. & Pichon, A. L. & Garces, M. & Fee, D. & Tsuyuki, T. & Watada, S. & Morii, W. 2008 Low-frequency acoustic-gravity waves from coseismic vertical deformation associated with the 2004 Sumatra-Andaman earthquake (Mw=9.2) *J. Geophys. Res.* **113**, B12402, doi:10.1029/2008JB005710

Watada, S. & Kunugi, T. & Hirata, K. & Sugioka, H. & Nishida, K. & Sekiguchi, S. & Oikawa, J. & Tsuji, Y. & Kanamori, H. 2006 Atmospheric Pressure Change Associated with the 2003 Tokachi-Oki Earthquake. *Geophys. Res. Lett.* **33**, L24306, doi:10.1029/2006GL027967.

Waxler, R. & Gilbert, K. E. 2006 The radiation of atmospheric microbaroms by ocean waves. *J. Acoust. Soc. Am.* **119**, 2651–2664.

Whitham, G. B. 1999 *Linear and Nonlinear Waves.* John Wiley & Sons.

Williams, W. G. 1999 *Fourier Acoustics.* Academic Press.

Yih, C.-S. 1980 *Stratified Flows.* Academic Press.